PHYSICAL REVIEW B VOLUME 43, NUMBER 16 1 JUNE 1991

Experimental and molecular-dynamics study of the Ar emission mechanism during low-energy Ar^+ bombardment of Cu

H. Feil, J. van Zwol, S. T. de Zwart, and J. Dieleman
Philips Research Laboratories, P.O. Box 80 000, 5600 JA Eindhoven, The Netherlands

B. J. Garrison
Department of Chemistry, The Pennsylvania State University, University Park, Pennsylvania 16802
(Received 19 November 1990)

Angle-resolved time-of-flight distributions of Ar atoms emitted during Ar^+ bombardment of Cu have been measured and compared to results of molecular-dynamics simulations. For keV incident energies, implanted Ar atoms escape peaked along the surface normal, due to a high excitation density of the surface, induced by a nearby Ar^+ impact and the negligible attraction between Ar and Cu. At low incident energies, the simulations show that the Ar is trapped for a short time in the first Cu layers, undergoes a few collisions and is emitted in a similar direction but at higher kinetic energy.

Recently, angle-resolved time-of-flight (ARTOF) data on sputtering of noble-gas atoms incorporated during erosion of solids by keV noble-gas ion bombardment have become available.[1,2] Three striking observations are made in these works on Ar^+ bombardment of Cu and Si. First, the time-of-flight (TOF) distributions of Ar consist of two components. Second, neither of these components can be fitted with a collision-cascade-like distribution, as is usual for sputtering of elements or alloys in this ion energy range.[3-5] However, the fast component is described well with a Maxwell-Boltzmann (MB) distribution at high temperature ($T \approx 2000$ K) on a constant stream velocity and the slow component by a MB distribution at approximately target temperature. And third, the fast component does not follow a cosinelike angular distribution, but shows a strongly over-cosine peaking along the surface normal.

The best fit to the ARTOF data of the slow component is obtained with a MB distribution and cosine angular dependence, even if the temperature is varied. Since the temperature derived from the MB fit also corresponds quite well to the target temperature, this slow component is identified with ion-bombardment-enhanced diffusion of implanted Ar to the surface and subsequent evaporation at the target temperature.

Most of the experiments have been performed at fluences where independent studies have shown considerable gas-bubble formation to occur.[6] This suggests that the fast component is due to Ar atoms expanding from gas bubbles opened by sputtering. This interpretation is supported by several observations, two of which will be mentioned here. First of all, the average kinetic energy of the fast Ar atoms lies in the range of values calculated for the average potential energy of the Ar atoms inside the bubbles.[1] Second, the ARTOF distributions observed for 3-keV Ar^+ sputtering of Ar from Cu have been fitted most satisfactorily by using an analytical model based on the assumption of Ar atoms expanding from a bubble analogous to expansion from a nozzle.[2]

In this paper, we demonstrate that recent experiments, particularly those performed at low Ar^+ incident energy, complemented by a molecular-dynamics simulation method capable of dealing with high ion doses, have shown that the fast component does not necessarily arise from gas bubbles as previously suggested,[1,2] but may be due to Ar atoms escaping from the solid through a region of the solid on top of them, a region which has been highly excited by an Ar^+ impact. This paper describes some of the crucial observations leading to this conclusion for Ar^+ bombardment of Cu. A description of the equipment may be found in earlier work.[2]

In the molecular-dynamics (MD) simulations a cubic [$V \approx (24\ \text{Å})^3$] microcrystallite of about 1300 Cu atoms with a (100) surface exposed is bombarded with Ar^+ ions. The Cu-Cu interactions are described by a pair potential of the type

$$V(r) = \begin{cases} A(Br^{-p} - r^{-q})\exp[C(r-a)^{-1}], & r < a \\ 0, & r \geq a \end{cases}$$

with the following values for the parameters: $A = 8.333$ eV $\text{Å}^{0.472}$, $B = 9.333$ $\text{Å}^{2.972}$, $C = 2.0$ Å, $p = 3.444$, $q = 0.472$, and $a = 4.0$ Å. The potential automatically cuts off at $r = a$. The potential is fitted to give the experimental cohesive energy of 3.49 eV per atom and the equilibrium lattice constant of 3.61 Å.[7] To incorporate a more repulsive Cu-Cu interaction at short internuclear separations, the potential is splined between $r = 1.03$ and $r = 1.53$ Å to a Moliere potential with a screening length of 0.83 times the Firsov value.[8] The attractive Ar-Ar and Cu-Ar interactions are negligible under the experimental conditions. The nonbonding Ar-Cu and Ar-Ar interactions are described by a Moliere potential, also with a screening length of 0.83 times the Firsov value. The potentials are cut off smoothly at 4 Å.

Usually, a set of trajectories is developed by uniform sampling of a representative area reflecting the underlying symmetry of the crystal.[9] With every new trajectory, a fresh surface is bombarded with the ion. This approach implies that a simulation is made of a low-dose experi-

ment. Sputtering of implanted Ar atoms cannot be simulated using this method.

In the present approach we bombard the crystallite continuously with Ar^+ ions without refreshing the lattice. This gives us the opportunity to study the implantation of more than one Ar atom in the crystallite and possible clustering of the Ar atoms. It also allows the implanted Ar atoms to escape due to a subsequent impact. Because the lattice is not refreshed, the symmetry is broken after the first impact and the experiments may be better compared with the simulations when the impact points are distributed over a larger surface area. Therefore the impact points of the incident Ar^+ ions are randomly taken within a radius of about 5 Å from the center of the surface. Energy distributions are obtained by averaging the results of 50 trajectories.

A problem would arise if we repeatedly supplied energy to the crystallite. The temperature of the finite crystallite would increase too much. A temperature control is added in order to avoid this problem. The method described by Berendsen *et al.*[10] is used to couple all the atoms of the crystallite to an external bath with constant temperature. In the simulation, the coupling is to a bath at $T=300$ K with a time constant $\tau=400$ fs. With this value the copper crystallite is cooled down to 300 K in about 3 ps after an impact of a 1-keV Ar^+ ion. As can be derived from the MD simulations of Hsieh *et al.*,[11] this seems to be a reasonable cooling rate. They studied the time dependence of the temperature of a very large copper crystallite where a keV cascade is simulated by assigning the entire energy to an interior atom in the large crystallite.

The preservation of the approximate shape of the crystallite is obtained by applying a removable boundary condition. Initially, all edge atoms of the crystallite, except, of course, those at the surface, are coupled to their initial positions with a harmonic force. The value of the force constant is 10^{-8} N m^{-1}. When a trajectory is completed, several Cu atoms may have been sputtered or may have escaped from the crystallite through the edges. With this boundary condition, it is obvious that after several impacts a pit, on a microscopic scale, is formed in the crystallite. It is not expected that such a pit will be present in the experimental situation. To deal with this simulation artifact, the boundary condition for the edge atoms positioned at the top of the side walls of the crystallite can be removed as soon as the crystallite contains less atoms after a trajectory than before the trajectory. These atoms are then allowed to participate in the relaxation process of the surface.

In order to obtain more information on the mechanism responsible for the fast peak in the TOF spectra, we experimentally varied the energy of the incident Ar^+ ions from $E_i=3$ keV to 200 eV and the dose between 10^{15} and 10^{19} Ar^+ cm^{-2}. The measured kinetic-energy distributions of the Ar atoms exiting along the surface normal ($\vartheta_0=0°$) are presented in Fig. 1 (only the fast peaks are displayed). It is clear that the distribution varies strongly with the incident ion energy. The mean energy of the emitted Ar atoms increases smoothly with decreasing Ar^+ ion energy. Except for the 3-keV ion energy, the $\vartheta_0=0°$

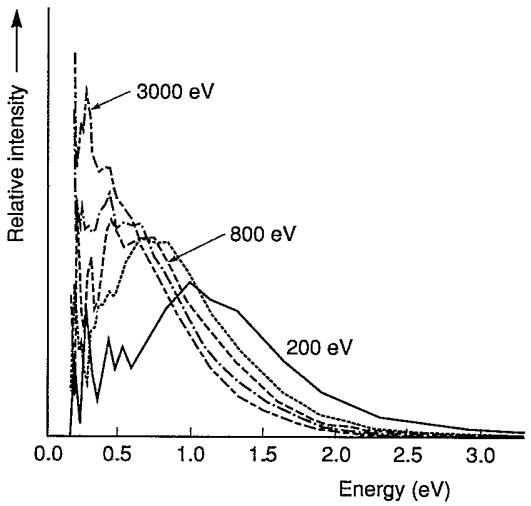

FIG. 1. Experimental energy distributions of resputtered Ar atoms for $\vartheta_0=0°$ exit angle. The ion energy is varied from $E_i=200$ eV to 3 keV. (——), 200 eV; (---), 400 eV; (— — —), 800 eV; (·---·), 1500 eV; and (—·—·—), 3000 eV. The structures in the distributions at the low-energy side are due to experimental noise.

energy distributions of the fast component deviate significantly from MB distributions. The slow peak, appearing in the $E_i=3$-keV TOF distributions,[2] has disappeared completely at $E_i=200$ eV.

The MD computer simulations on the sputtering of the Ar atoms from Cu are performed with an angle of incidence of $\vartheta_i=0°$ and Ar^+ incident ion energies $E_i=1000$, 200, and 40 eV, and also $\vartheta_i=50°$ with $E_i=200$ and 40 eV. Simulations performed with an angle of incidence of $\vartheta_i=50°$ indicate that for $E_i=200$ eV or higher, the energy distributions do not deviate much from the $\vartheta_i=0°$ case. For $E_i=40$ eV, the mean energy of the emitted atoms is much higher with $\vartheta_i=50°$. Since the emission mechanisms, for the cases which we can compare with the experiments, are found to be rather insensitive to the variation of the angle of incidence, only results for $\vartheta_i=0°$ are presented here. Figure 2 depicts calculated energy distributions of Ar atoms escaping from the surface during Ar^+ ion bombardment. It is clear that at high ion energies, a relatively large fraction of the Ar atoms escapes from the surface with a low energy. As the ion energy decreases, the mean energy of the escaping atoms increases. It is also found that the distributions are peaked along the surface normal, as measured for the $E_i=3$-keV experiments.

From a comparison of Figs. 1 and 2, it follows that the results of the MD simulations are, even semiquantitatively, equivalent to the experimental results. This means that a detailed analysis of the simulations can be very helpful in understanding the mechanisms that lead to the measured angle-resolved energy distributions.

The simulation at $E_i=1000$-eV incident Ar^+ ion energy will be discussed first. The Ar^+ creates heavy damage while it deposits a considerable amount of its energy in the top layers of the crystallite. Most sputtered Cu atoms leave early in the cascade, up to about 200 fs. After about

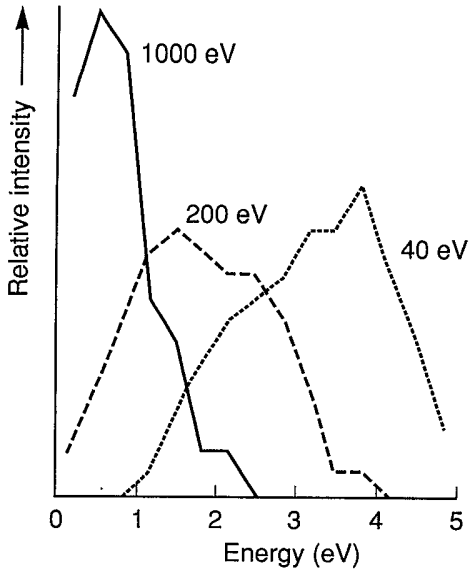

FIG. 2. Energy distributions of sputtered Ar atoms obtained from MD simulations. $E_i = 1000$, 200, and 40 eV.

200 fs, all the atoms in the crystallite are moving. Subsequently, cooling due to the coupling to the external bath with temperature $T = 300$ K takes over. Ar atoms are mainly implanted 10 to 20 Å below the surface. As soon as more Ar atoms are implanted, clusters of Ar are formed within the implantation region. In our simulation, we found single Ar atoms and clusters of up to about 5 Ar atoms; however, the statistics are not sufficiently good to predict an exact maximum cluster size.

When, during a subsequent impact, a considerable amount of the primary ion energy is deposited above an implanted Ar atom or an Ar cluster, the damage and high excitation density in this region enables the implanted Ar atom(s) to diffuse through this highly excited region towards the surface. Because of the nonbonding character of Ar-Cu interaction, the Ar atoms have a large probability of escaping from the surface. Even though in the real system there is a slight attractive interaction, it is negligible compared to the interactions in the bombarded substrate. The peaking of the velocities along the surface normal is due to the direction of the diffusion along the density gradient towards the surface. The Ar atoms escape much later than the sputtered Cu atoms: $t > 2$ ps compared to $t < 200$ fs for the sputtered Cu atoms. It is clear that at $t > 2$ ps, no atoms in the crystallite are present with a high kinetic energy. Thus, the kinetic-energy distribution will not contain a high-energy contribution.

About 10% of the incident Ar atoms escape through the bottom of the crystallite. We are not able to simulate the behavior of these atoms. Maybe they are responsible for the observed bubbles in the transmission-electron-microscopic measurements. The formation of these Ar bubbles is expected to take place on longer time scales.

An analysis of the simulation of the $E_i = 200$-eV experiment shows that the emission mechanism is very different from that for the $E_i = 1000$-eV case. The incident Ar^+ ion only penetrates into the first few surface layers. Due to the excitation of the surface layer and the nonbonding character of the Ar-Cu interaction, the Ar atom escapes from the surface within about 200 fs. This means that no Ar atoms are implanted, completely consistent with earlier observations.[12] This is also the reason why the slow peak in the experimental TOF distributions disappears at low ion energies.

The relatively large excitation density of the surface layer at the moment of escape of an Ar atom after the 200-eV impact results in an increased mean energy of the escaping Ar atoms compared to the $E_i = 1000$-eV case. To investigate the tendency of increasing energy of escaping atoms with decreasing incident ion energy, simulations are performed with $E_i = 40$-eV ion energy. This tendency is clearly visible in Fig. 2, the mean energy of the escaping Ar atoms at $E_i = 40$ eV is about twice the mean energy of the Ar atoms at $E_i = 200$ eV.

Summarizing, the smooth increase of the mean kinetic energy of the emitted Ar atoms with decreasing Ar^+ incident energy down to $E_i = 200$ eV where entrapment of Ar in Cu is negligible, as well as the strong peaking of the angular distribution along the surface normal observed already at doses where bubble formation is expected to be negligible, definitively show that the fast component in the TOF spectra can be explained by a more general mechanism than opening of Ar bubbles by sputter erosion. The results of MD simulations are consistent with the experimental results over the whole range of values of Ar^+ dose and incident energy. In addition, these MD simulations show that at high Ar^+ incident energies the high excitation density caused by an Ar^+ impact in a volume ranging down to the implantation depth, enables Ar atoms, implanted in earlier impacts (or the implanting atom itself), to escape through this region to the surface. The high kinetic energy and the directionality along the surface normal are imparted to the Ar atoms in collisions with the Cu atoms in the highly excited volume on their way to the surface; this causes the nozzlelike behavior. For low E_i (≤ 200 eV), where implantation does not occur, the MD simulations for $\vartheta_i = 0°$ show that the Ar is trapped for a very short time in the very first atomic Cu layers, suffers a few collisions, and is emitted with kinetic energies and directionality quite similar to those at higher E_i. This also explains why the slow component in the TOF distributions is no longer observed for $E_i = 200$ eV.

The reported mechanisms are rather insensitive for variations in the interatomic potentials. Experimentally, this is confirmed by the observation of similar behavior for different noble gases and other elements.[13]

[1]G. N. A. van Veen, F. H. M. Sanders, J. Dieleman, A. van Veen, D. J. Oostra, and A. E. de Vries, Phys. Rev. Lett. **57**, 739 (1986).

[2]J. van Zwol, S. T. de Zwart, C. G. A. Busquet, and J. Dieleman, Appl. Surf. Sci. **43**, 363 (1989).

[3]*Sputtering by Particle Bombardment I,* edited by R. Behrisch, Topics in Applied Physics Vol. 47 (Springer, Berlin, 1981).

[4]J. P. Baxter, J. Singh, G. A. Schick, P. H. Kobrin, and N. Winograd, Nucl. Instrum. Methods Phys. Res. Sect. B **17**, 300 (1986).

[5]B. J. Garrison, Nucl. Instrum. Methods Phys. Res. Sect. B **17**, 305 (1986).

[6]U. Bangert, P. J. Goodhew, C. Jeynes, and I. H. Wilson, J. Phys. D **19**, 589 (1986).

[7]*Handbook of Chemistry and Physics,* 70th ed. (Chemical Rubber, Cleveland, Boca Raton, 1990).

[8]I. M. Torrens, *Interatomic Potentials* (Academic, New York, 1972).

[9]D. E. Harrison, Crit. Rev. Solid State Mater. Sci. **14**, S1 Suppl. 1 (1988).

[10]H. J. C. Berendsen, J. P. M. Postma, W. F. van Gunsteren, A. DiNola, and J. R. Haak, J. Chem. Phys. **81**, 3684 (1984).

[11]Horngmieh Hsieh, T. Diaz de la Rubia, R. S. Averback, and R. Benedek, Phys. Rev. B **40**, 9986 (1989).

[12]A. O. R. Cavaleru, C. M. Morley, D. G. Armour, and G. Carter, Radiat. Eff. **18**, 87 (1973).

[13]J. van Zwol and S. T. de Zwart (unpublished).